Biol Cybern (2011) 105:21–27
DOI 10.1007/s00422-011-0447-5

ORIGINAL PAPER

Biological Cybernetics

Network model of chemical-sensing system inspired by mouse taste buds

Katsumi Tateno · Jun Igarashi · Yoshitaka Ohtubo · Kazuki Nakada · Tsutomu Miki · Kiyonori Yoshii

Received: 9 September 2010 / Accepted: 29 June 2011 / Published online: 14 July 2011

Abstract Taste buds endure extreme changes in temperature, pH, osmolarity, so on. Even though taste bud cells are replaced in a short span, they contribute to consistent taste reception. Each taste bud consists of about 50 cells whose networks are assumed to process taste information, at least preliminarily. In this article, we describe a neural network model inspired by the taste bud cells of mice. It consists of two layers. In the first layer, the chemical stimulus is transduced into an irregular spike train. The synchronization of the output impulses is induced by the irregular spike train at the second layer. These results show that the intensity of the chemical stimulus is encoded as the degree of the synchronization of output impulses. The present algorithms for signal processing result in a robust chemical-sensing system.

Keywords Chemical sensor array · Taste bud · Spiking neural network · Synchronization

1 Introduction

Taste bud cells sense taste. The oral cavity is not a good environment for taste bud cells. A fall in pH or a sudden change in temperature often occurs in the oral cavity. The taste bud cells work properly under such unpleasant environments. The turnover of taste bud cells occurs in a short period (Beidler 1970; Farbman 1980). A fatigued taste bud cell is replaced with a new one that may not have identical sensitivity. Although the turnover may cause inconsistent sensitivity for taste reception, taste is consistently recognized in this chemical-sensing system with non-identical sensing units. Such ability is beneficial for a chemical-sensing device in engineering.

Each taste bud consists of several tens of cells, which are classified into types I to IV (Lindemann 1996). Each cell type is assigned to different roles. Type II and III cells have taste receptors. Type I and IV cells are considered to be supportive cells and precursors of the other cell types, respectively. Type II cells are constituted of about 10 cells in a taste bud on mouse fungiform papillae (Ohtubo 2007; Ohtubo and Yoshii 2011). The number of type III cells is about two in a fungiform taste bud (Ohtubo 2007; Ohtubo and Yoshii 2011). Type III cells make synaptic contacts with nerve terminals (Seta and Toyoshima 1995) and are considered output cells that relay the identity and intensity of chemical stimuli to the brain. Type II cells do not have synaptic contacts with taste nerves. Signal transmission from Type II cells to Type III cells is necessary for taste signal processing. Type II cells release ATP (Huang et al. 2007; Dando and Roper 2009). ATP stimulates other taste cells to release serotonin, which causes responses of afferent taste fibers. Further, mouse Type III cells have ATP receptors (Kataoka et al. 2004). This indicates cell-to-cell communication in taste buds.

An improvement in signal sensing by noise in mechanical or electric receptor cells has been reported (Douglass et al. 1993; Moss et al. 1994; Braun et al. 1994; Levin and Miller 1996; Freund et al. 2002; Neiman and Russell 2002; Galán et al. 2006). The hair mechanoreceptor in the crayfish tail fan is specialized for the detection of small-amplitude water motions (Wilkens and Douglass 1994). In the presence of noise, the sum of the subthreshold signal and

K. Tateno (✉) · Y. Ohtubo · K. Nakada · T. Miki · K. Yoshii
Department of Brain Science and Engineering, Kyushu Institute of Technology, 2-4 Hibikino, Wakamatsu-ku, Kitakyushu 808-0196, Japan,
e-mail: tateno@brain.kyutech.ac.jp

J. Igarashi
Computational Science Research Program, Integrated Simulation of Living Matter Group, Brain and Neural Systems Team, RIKEN, 2-1 Hirosawa, Wako, Saitama 351-0198, Japan

the noise generates an action potential in sensory neurons (Douglass et al. 1993). Noise-induced synchronization in a pair of uncoupled non-identical electroreceptors exists in paddlefish (Neiman and Russell 2002). In noise-induced synchronization, Gaussian noise induces the synchronization of bursts in a pair of uncoupled electroreceptors. A stochastic process encodes sensory input to neural spikes, and signal-encoding algorithms via the stochastic process could be introduced into a chemical-sensing system.

We describe here a signal-processing algorithm for a chemical-sensing system in which the intensity of the chemical stimulus is transduced into a neural spike train. The design of the present chemical-sensing system was inspired by mice taste bud cells and consists of two layers: a Type II cell layer and a Type III cell layer. Spike synchronization induced by a random signal transmission was considered at the Type III cell model layer. The intensity of the chemical stimulus was encoded as a degree of the synchronization of the output impulses.

2 Methods

A schematic diagram of the present chemical-sensing system is shown in Fig. 1. It consists of 10 Type II and 2 Type III cell models. There was no connection among the Type II cell models. It is assumed that the Type II cell models received chemical substances. A receptive membrane will be introduced as a branch of the Type II cell models. A chemical stimulus increased the input resistance of the Type II cell models and led to depolarization of the membrane potentials. When the Type II cell models fired, action potentials were converted to telegraph pulses. The telegraph pulse trains derived by the Type II cell models were superposed. The resulting sum of the telegraph pulse trains converged equally on the Type III cell models. The common telegraph pulses elevated the membrane state variables of the Type III cell models. When the membrane state variables reached the threshold, output impulses were generated, and the degree of synchronization between output impulse trains was evaluated.

2.1 Type II cell model

Ionic currents of mouse Type II taste cells are primarily transient sodium and outward rectifier currents (Kimura et al. 2007). The outward rectifier currents consist of ATP efflux mediated by ATP-permeable channels whose reversal potential is near 0 mV (Romanov et al. 2008). The ATP-permeable channels are slowly activating and deactivating channels. Those indicate that the ATP current contributes less to shaping action potentials. For simplicity, the outward current was replaced with a passive current. We used a transient sodium model (Izhikevich 2007) as the Type II cell model consisting of transient sodium and leak currents:

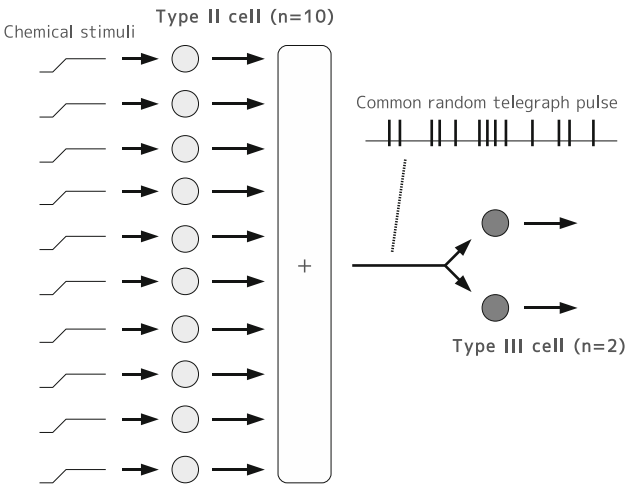

Fig. 1 Schematic diagram of chemical-sensing system. The chemical-sensing system consists of 10 Type II cell models and 2 uncoupled Type III cell models

$$C_{\mathrm{m}}\frac{\mathrm{d}v_i}{\mathrm{d}t} = -\bar{g}_{\mathrm{Na}}m_{\infty,i}^3 h_i(v_i - e_{\mathrm{Na}}) - g_{\mathrm{l}}(v_i - e_{\mathrm{l}}) + \xi_i(t) \tag{1}$$

$$\frac{\mathrm{d}h_i}{\mathrm{d}t} = \frac{h_{\infty,i} - h_i}{\tau_h(v_i)}, \tag{2}$$

where $i = 1, 2, \ldots, 10$. g_{l} is the leak conductance. Input to the Type II cells was fed to g_{l}. The modulation of g_{l} changed the input resistance of the Type II cells. The parameters were fixed at $C_{\mathrm{m}} = 1\ \mu\mathrm{F/cm}^2$, $e_{\mathrm{Na}} = 60$ mV, $e_{\mathrm{l}} = -60$ mV, and $\bar{g}_{\mathrm{Na}} = 15\ \mathrm{mS/cm}^2$. $\xi_i(t)$ is the Gaussian noise. $<\xi_i(t)\xi_i(t')>= \sigma_{\mathrm{nat}}^2\delta(t-t')$. $\sigma_{\mathrm{nat}} = 2\ \mathrm{mV\ ms}^{-1/2}$ unless otherwise specified.

The rate function of the sodium current is:

$$m_\infty(v_i) = \frac{1}{1 + \exp((-40 - v_i)/9)} \tag{3}$$

$$h_\infty(v_i) = \frac{1}{1 + \exp((62 + v_i)/7)} \tag{4}$$

$$\tau_h(v_i) = 1.2 + \tau_{\mathrm{amp}} \cdot \exp\left(-\frac{(-67 - v_i)^2}{400}\right). \tag{5}$$

Inactivation variable h_i of the sodium current has a voltage-dependent time constant. The mouse taste receptor cells take ~1 s for recovery from inactivation (Ohtubo et al. 2008; Ohtubo 2009). That time constant is roughly 100 times larger than the typical value reported by Izhikevich (2007). Here, $\tau_{\mathrm{amp}} = 740$ ms.

The synaptic input to the Type III cell models was given by the sum of the spike trains derived by the Type II cell models. The sum of many independent spike trains has an exponential distribution of interspike intervals. A single Type II cell model randomly elicited spike trains of action potential. The interspike interval distribution was skewed to the right at g_{l} of 0.8 $\mathrm{mS/cm}^2$. By adding 10 spike trains, an exponential-like

distribution was obtained. A spike train derived by 10 independent Type II cell models had sparse or dense interspike intervals. The mean coefficient of the variation was 0.9 at g_l of 0.8 mS/cm^2.

2.2 Type III cell model

Electrophysiological properties of Type III cells are still unknown. Mouse Type III cells have transient sodium currents and outward rectifier potassium currents (Kimura et al. 2007). The outward rectifier currents are TEA-sensitive potassium currents, which cause quick repolarization after excitations. Type III taste cells are likely to be a spiking neuron. The present Type III cell model is part of a canonical phase model proposed by Neiman and Russell (2002). The Gaussian noise drives the qualitative changes in the firing pattern of their single neurons and changes from a quasiperiodic to a bursting mode. In a pair of non-identical uncoupled neuron models, the synchronization of noise-induced bursts is induced. The slow dynamics of the canonical phase model works as a key for noise-induced synchronization.

The Type III cell model is the slow dynamics of the canonical phase model of Neiman and Russell (2002):

$$\varepsilon \frac{\mathrm{d}\psi_j}{\mathrm{d}t} = 1 - \epsilon \sin \psi_j(t) + s(t) + \zeta_j(t) \quad (j = 1, 2)\,, \qquad (6)$$

where $\varepsilon = 20$ ms and $\epsilon_1 = \epsilon_2 = 1.1$. The cells are identical. If membrane state variable ψ reaches or exceeds threshold value $2\,\pi$, the cells fire, producing an output event. The form of the action potential was not explicitly described. Immediately after that, ψ resets to 0. ζ_j is the Gaussian noise. $< \zeta_j(t)\zeta_j(t') > = \sigma_c^2 \delta(t - t')$. $\sigma_c = 0.005$ ms$^{-1/2}$ unless otherwise specified.

The telegraph pulse input was given by $s(t)$. The telegraph pulse fluctuates between 0 and 1. In Sect. 3.1, the random telegraph pulse was applied as $s(t)$. The duration of the pulse was fixed at 5 ms. Jumps from 0 to 1 occurred randomly. In Sect. 3.3, the telegraph pulse was derived by an array of Type II cell models.

The Type III cell model has a single shallow potential well in which membrane state value ψ stays constant. The bottom of the potential well is at $\psi^* = \sin^{-1}(1/\epsilon)$, which is a stable fixed point. During $s(t) = 1$, the stable fixed point disappears by saddle-node bifurcation. The potential slope becomes a monotonous decremental function, and then ψ moves along the potential slope. If the pulse duration is sufficiently long, ψ reaches 2π, and the Type III cell model fires. If ψ fails to reach the threshold value, ψ returns to the stable fixed point. In this study, the intensity of $s(t)$ was 1, and the duration of the random telegraph pulse was 5 ms, which is below the strength–duration curve of the Type III cell model. The strength–duration curve is the relation between the strength of the applied current and the time it takes for ψ to get from ψ^* to the firing threshold. Membrane state variable ψ does not overshoot the threshold by a single telegraph pulse. Two or more successive pulses are necessary for excitation.

2.3 Computer simulation

Before simulations of the Type II–Type III network model, we separately simulated the Type II and Type III networks. First, a pair of uncoupled Type III cell models was stimulated by the random telegraph pulse that was equally given to the Type III cell models. The interpulse intervals of the random telegraph pulse were drawn from an exponential distribution. Jumps from 0 to 1 occurred randomly. The mean interpulse interval T was varied. The pulse duration was fixed at 5 ms.

In addition, a pair of Type III cell models was stimulated by the periodic telegraph pulse. The robustness of the synchronization of the output impulses to the noise intensity was assessed.

The degree of the synchronization of the output impulses in the Type III cell pair was quantified by the following equation:

$$\gamma^2 = < \sin \Delta\phi >^2 + < \cos \Delta\phi >^2 \ , \qquad (7)$$

where $\Delta\phi$ is the phase difference between the cells. The brackets denote the average over time. The phase $\phi_j(t)$ of impulse trains in each Type III cell ($j = 1, 2$) increased by 2π every time an impulse occurred, and was interpolated linearly between sequential impulses. For an evaluation of γ, at least 20 impulses were used. Assessment by a few impulses caused overestimation of γ. The synchronization index is also known as the vector strength.

Second, the sum of the independent spike trains derived by an array of Type II cell models was obtained. No interaction between the Type II cell models existed. The mean interspike interval of the sum of the spike trains was obtained. Spikes of 10^3 were collected at incremental step g_ls, which ranged between 0.15 and 1.0 mS/cm^2. The mean value and the standard deviation of the interspike intervals were calculated, as well as the coefficient of variation.

In the Type II–Type III network model, we assumed that leak conductance g_l declined with the intensity of the chemical stimulus. The Type II cell model generated a random telegraph pulse. The spiking frequency of the Type II cell model was dependent on g_l. An action potential was converted to a telegraph pulse. The membrane potential of the Type II cells was first converted to a telegraph pulse $s_i(t)$ ($i = 1, 2, \ldots, 10$) via the Heaviside function $\theta(v_i(t) - 40)$. Those telegraph pulses were superposed:

$$s(t) = \begin{cases} 1 & \text{if } s_i(t) = 1 \text{ for any } i = 1,\ldots,10, \\ 0 & \text{otherwise.} \end{cases} \qquad (8)$$

The resulting sum of the telegraph pulse trains was commonly inputted to the Type III cell models. The common

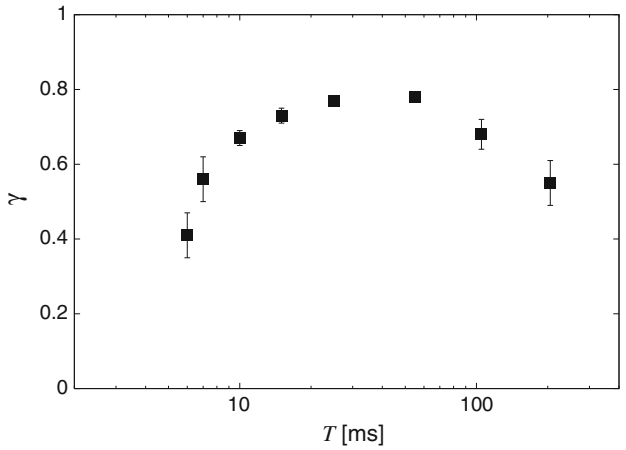

Fig. 2 Synchronization of impulses induced by the random telegraph pulses in a pair of uncoupled Type III cell models. γ was ~0.8 around the mean interpulse interval $T = 50$ ms

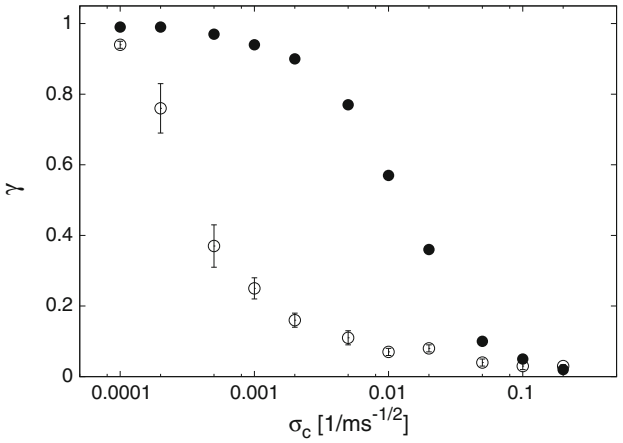

Fig. 3 Robust synchronization by the random telegraph pulse in a pair of uncoupled Type III cell models. *filled circle*: random telegraph pulse. Mean interval = 50 ms. *Unfilled circle*: periodic telegraph pulse. Pulse interval = 50 ms

telegraph pulse train elicited impulses of the Type III cell model. The degree of synchronization of the output impulses in a pair of Type III cell models was assessed by Eq. 7.

3 Results

3.1 Stochastic synchronization of impulses in a pair of uncoupled Type III cell models

The common random telegraph pulse train simultaneously elicited impulses in the Type III cell models. High synchronization index was observed in the pulse interval range between 20 and 100 ms (Fig. 2). When the telegraph pulses successively occur, the Type III cells tend to elicit a spike simultaneously. By shortening the mean interpulse interval T, bursts of the telegraph pulses increased. Consequently, the synchronization index improved to $T = \sim 20$ ms. In the range of T below 20 ms, membrane state variable ψ was frequently depolarized and hardly stayed near the stable fixed point. Such fluctuations lowered the degree of the synchronization of the impulses. Further, a continuous depolarization step current led to a low synchronization index (data not shown). The synchronization of the output impulses was facilitated by a pause between bursts of telegraph pulses.

The random telegraph pulse led to more robust synchronization in a pair of uncoupled Type III cell models than the periodic telegraph pulse in the presence of noise (Fig. 3). The Gaussian noise introduced unpaired impulses and lowered the degree of the synchronization of the impulses in both cases. The weak noise did not disturb synchronization of the Type III cell pair in either the periodic or random drives. For the random telegraph pulses, the rate of decrement was less steep. When the noise was relatively strong, the phase difference $\Delta\phi$ appeared as a sequence of rapid jumps. Constant values of $\Delta\phi$ were more likely to be observed. Therefore, the synchronization index remained high. For the periodic telegraph pulse trains, the noisy phase dynamics were found. The phase differences were broadly distributed between 0 and 2π. Thereby, the synchronization index became low.

3.2 Telegraph pulses generated by array of Type II cell models

The sum of the spike trains derived by an array of Type II cell models had an exponential-like distribution of interspike intervals. The coefficient of the variation of the interval density was ≥ 0.9 in the range of g_l between 0.15 and 1.0 mS/cm^2. The mean interval of the sum of the spike trains depended on leak conductance g_l (Fig. 4). The mean interval decreased with a decrease in g_l. As the decrease in g_l lowered the potential barrier for excitation, the mean interval was shortened. In the range of g_l below 0.7 mS/cm^2, the mean interval was shorter than 100 ms. The array of the Type II cell models potentially induces a high degree of synchronization of output impulses in a pair of Type III cell models in the range of g_l below 0.7 mS/cm^2.

3.3 Spike synchronization in Type II—Type III network model

An array of Type II cell models is commonly connected with Type III cell models. The superposition of spike trains derived by Type II cell models worked as common random telegraph pulses. The common random telegraph pulse induced the synchronization of output impulses. Synchronization index γ is summarized in Fig. 5. The synchronization of output impulses was facilitated with a decrease in g_l. Further, the frequency of the output impulses increased. Those results

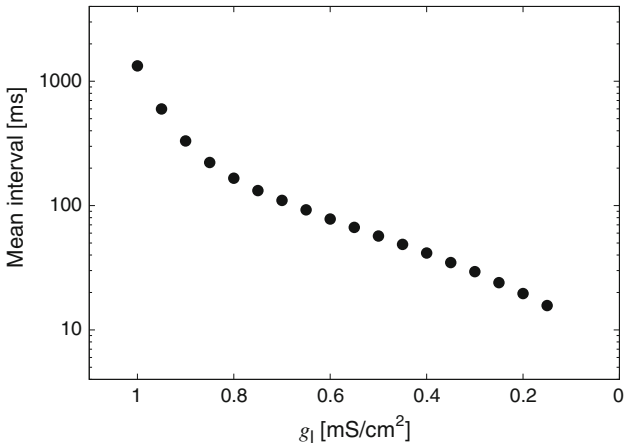

Fig. 4 Mean interval of superimposed spike train derived by an array of 10 Type II cell models. The abscissa is in reverse order

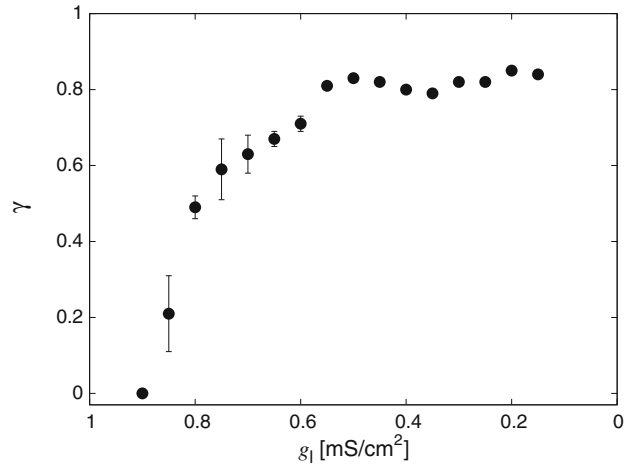

Fig. 5 Synchronization index in the Type II–Type III network model. Synchronization index γ in a pair of uncoupled Type III cell models was plotted as a function of g_I of Type II cell models. γ monotonically increased with a decrease in g_I. The abscissa is in reverse order

imply that the intensity of the chemical stimulus can be represented by the degree of the synchronization of the output impulses. When $g_I = 0.85$ mS/cm^2, the synchronization index was occasionally overestimated due to a low frequency (<0.005 Hz). This caused a large error bar.

4 Discussion

Our present chemical-sensing system proposed a signal transduction from the intensity of the chemical stimulus into the degree of synchronization of neural spikes. The intensity of the chemical stimulus was converted into a random telegraph pulse train. Those random telegraph pulses induced the synchronization of the output impulses in uncoupled excitable cells. Consequently, the intensity of the chemical stimulus was encoded by the degree of synchronization of the output impulses.

Synchronization of output impulses between the Type III cells is a working hypothesis. However, two experimental results support our hypothesis. First, in an experiment on voltage-sensitive dye, taste stimulation induced synchronized depolarization (or hyperpolarization) of taste bud cells (Ohtubo et al. 2001). Second, there are paracrinic systems in taste buds. The chemical transmitter is released into the extracellular space among taste bud cells. Such chemical transmission may elicit simultaneous neural activity in the Type III cells.

The synchronization of uncoupled oscillators induced by common noise is known as noise-induced synchronization. Common random telegraph pulses can also induce the synchronization of uncoupled nonlinear oscillators (Nagai et al. 2005; Nagai and Nakao 2009). The common random telegraph pulse induced the synchronization of impulses in a pair of uncoupled Type III cell models in this study. The Type III cell model is not in the oscillatory mode, but in an excitable state. While $s(t) = 0$, membrane state variable ψ stays near the fixed point in the presence of weak noise. The common telegraph pulse simultaneously stimulates both Type III cell models. Therefore, output impulses simultaneously occur in a pair of Type III cell models.

The intensity of the present telegraph pulse was below the strength–duration curve of the Type III cell model. A single telegraph pulse does not elicit an impulse in the Type III cell model. Two or more successive pulses are needed for impulse generation in the Type III cell model. On the other hand, the synchronization index was high in the range of mean interval T between 20 and 100 ms. Short interpulse intervals ($T < 20$ ms), however, decreased the degree of synchronization of the output impulses. While high frequency inputs increased the spiking frequency, such frequent depolarizations rather disturbed simultaneous spiking. Membrane state variable ψ returns at pauses between depolarization pulses. An adequate pause of the telegraph pulses facilitates the synchronization of the output impulses in the Type III cell pair.

As mentioned, a burst-like telegraph pulse train efficiently induces the synchronization of impulses in uncoupled Type III cell models. Such burst-like telegraph pulses were drawn from the exponential distribution of interpulse intervals. An exponential-like interpulse interval distribution emerges from the sum of independent pulse trains. A single Type II cell model has a right-skewed interval distribution. The interval distribution derived by the sum of spike trains does not depend on the exact spiking times of each spike train. Such random spike trains are consistently derived by the Type II cell model network. This suggests that a fatigued sensor is simply replaced with a new one in a chemical-sensing system.

As shown in Fig. 3, the random drives caused robust synchronization of impulses in a pair of the Type III cell models. When the Gaussian noise was relatively strong, the phase difference between the Type III cell models appeared as a sequence of rapid jumps. This is the phase slip. The phase differences were kept small. The phase slip is found in noisy systems in which a particle moves in a tilted potential with local minima (Pikovsky et al. 2001). Those local minima appear every 2π. The Type III cell models also have a tilted potential with local minima in the absence of telegraph pulse drives. The telegraph pulses shallow out potential wells. When impulses occur, the membrane state variable ψ jumps to next potential wells. If ψs stay near local minima, jumps coincidentally occur. As a single telegraph pulse is too weak to elicit an impulse, several successive pulses are needed to elicit an impulse. In the case of the random telegraph pulse train, a volley of the telegraph pulses elicits impulses of the Type III cells. In between the pulse volleys, ψs stay at the local minima in the potential. Therefore, certain values of the phase difference were observed. On the other hand, the periodic telegraph pulses elicited impulses that were entrained by the input telegraph pulses in the absence of the Gaussian noise. It was 1:n phase-locking. Those phase-locks were weak to the noise. Consequently, the phase differences exhibited noisy dynamics.

Mouse taste bud cells are not fast-spiking (Noguchi et al. 2003). The step current elicits a single spike or a few spikes at the beginning of the stimulus. The slow recovery from inactivation of the sodium channel causes long pauses of interspike intervals of taste bud cells. The present Type II cell model possesses slow recovery from sodium inactivation. The interval density of a single Type II cell model had a gamma-like distribution with long intervals. This causes a long interval in the sum of the spike trains derived by an array of Type II cell models. As a result, the common telegraph pulse exhibits stochastic alternations between 0 and 1 with adequate pauses.

The present chemical-sensing system will be involved in the cascade of layers in a neural network that ultimately classifies tastes. Sensory information is processed through a chain of diverging/converging links. A synchronous volley in the chemical-sensing system elicits a synchronous volley in the next layer. If synchronous transmissions of neural activity from layer to layer, such as a synfire chain (Abeles 1991), are assumed, the present chemical-sensing system can be the first layer of a neural network model for taste reception.

Acknowledgment This study was supported by a COE program (center #J19) granted to Kyushu Institute of Technology by MEXT of Japan.

References

Abeles M (1991) Corticonics. Cambridge University Press, Cambridge

Beidler LM (1970) Physiological properties of mammalian taste receptors. In: Wolstenholme GEW, Knight J (eds) Taste and smell in vertebrates. Churchill, London pp 51–67

Braun HA, Wissing H, Schäfer K, Hirsch MC (1994) Oscillation and noise determine signal transduction in shark multimodal sensory cells. Nature 367:270–273

Dando R, Roper SD (2009) Cell-to-cell communication in intact taste buds through ATP signalling from pannexin 1 gap junction hemichannels. J Physiol 587(24):5899–5906

Douglass JK, Wilkens L, Pantazelou E, Moss F (1993) Noise enhancement of information transfer in crayfish mechnoreceptors by stochastic resonance. Nature 365:337–340

Farbman AI (1980) Renewal of taste bud cells in rat circumvallate papillae. Cell Tissue Kinet 13:349–357

Freund JA, Schimansky-Geier L, Beisner B, Neiman A, Russell DF, Yakusheva T, Moss F (2002) Behavioral stochastic resonance: how the noise from a daphnia swarm enhances individual prey capture by juvenile paddlefish. J Theor Biol 214:71–83

Galán RF, Ermentrout GB, Urban NN (2006) Reliability, discriminability and stochastic synchronization of olfactory neurons. Sens Actuators B 116:168–173

Huang YJ, Maruyama Y, Dvoryanchikov G, Pereira E, Chaudhari N, Roper SD (2007) The role of pannexin 1 hemichannels in ATP release and cell-cell communication in mouse taste buds. Proc Natl Acad Sci USA 104(15):6436–6441

Izhikevich EM (2007) Dynamical systems in neuroscience. MIT Press, Cambridge

Kataoka S, Toyono T, Seta Y, Ogura T, Toyoshima K (2004) Expression of $P2Y_1$ receptors in rat taste buds. Histochem Cell Biol 121: 419–426

Kimura K, Ohtubo Y, Kumazawa T, Yoshii K (2007) Electrophysiological identification of mouse taste bud cells. Int Congr Ser 1301:254–257

Levin JE, Miller JP (1996) Broadband neural encoding in the cricket cercal sensory system enhanced by stochastic resonance. Nature 380:165–168

Lindemann B (1996) Taste reception. Physiol Rev 76:719–766

Moss F, Pierson D, O'Gorman D (1994) Stochastic resonance: tutorial and update. Int J Bifurc Chaos 4:1383–1397

Nagai K, Nakao H (2009) Experimental synchronization of circuit oscillations induced by common telegraph noise. Phys Rev E 79:036205

Nagai K, Nakao H, Tsubo Y (2005) Synchrony of neural oscillators induced by random telegraphic currents. Phys Rev E 71:036217

Neiman AB, Russell DF (2002) Synchronization of noise-induced bursts in noncoupled sensory neurons. Phys Rev Lett 88(13): 138103

Noguchi T, Ikeda Y, Miyajima M, Yoshii K (2003) Voltage-gated channels involved in taste responses and characterizing taste bud cells in mouse soft palates. Brain Res 982:241–259

Ohtubo Y (2007) Quantitative study on cell types in adult mouse taste buds. Int Congr Ser 1301:250–253

Ohtubo Y (2009) Voltage-gated sodium currents of cell types in mouse taste bud cells. In: Abstract of The 7th international symposium on molecular and neural mechanisms of taste and olfactory perception, p 28

Ohtubo Y, Yoshii K (2011) Quantitative analysis of taste bud cell numbers in fungiform and soft palate taste buds of mice. Brain Res 1367:13–21

Ohtubo Y, Suemitsu T, Shiobara S, Matsumoto T, Kumazawa T, Yoshii K (2001) Optical recordings of taste responses from fungiform papillae of mouse in situ. J Physiol 530:287–293

Ohtubo Y, Hashiba Y, Kimura K, Kumazawa T, Yoshii K (2008) Voltage-gated Na^+ currents of each cell type in mouse taste bud. In: Abstract of 18th congress of the European chemoreception research organization, p 83

Pikovsky A, Rosenblum M, Kurths J (2001) Synchronization. Cambridge University Press, Cambridge

Romanov RA, Rogachevskaja OA, Khokhlov AA, Kolesnikov SS (2008) Voltage dependence of ATP secretion in mammalian taste cells. J Gen Physiol 132(6):731–744

Seta Y, Toyoshima K (1995) Three-dimensional structure of the gustatory cell in the mouse fungiform taste buds: a computer-assisted reconstruction from serial ultrathin sections. Anat Embryol 191:83–88

Wilkens LA, Douglass JK (1994) A stimulus paradigm for analysis of near-field hydrodynamic sensitivity in crustaceans. J Exp Biol 189:263–272